

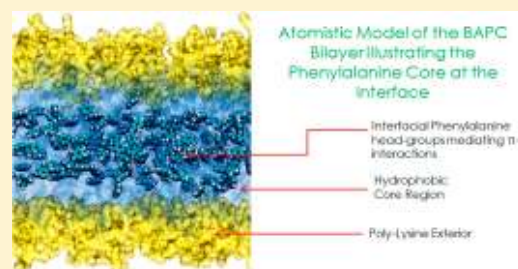
# Thermally Induced Conformational Transitions in Nascent Branched Amphiphilic Peptide Capsules

Pinakin Sukthankar, Susan K. Whitaker, Macy Garcia, Alvaro Herrera, Mark Boatwright, Om Prakash, and John M. Tomich\*

Department of Biochemistry and Molecular Biophysics, Kansas State University, Manhattan, Kansas 66502, United States

## Supporting Information

**ABSTRACT:** Branched amphiphilic peptide capsules (BAPCs) are biocompatible, bilayer delimited polycationic nanospheres that spontaneously form at room temperature through the coassembly of two amphiphilic branched peptides: bis(FLIVI)-K-K<sub>4</sub> and bis(FLIVIGSII)-K-K<sub>4</sub>. BAPCs are readily taken up by cells in culture, where they escape and/or evade the endocytic pathway and accumulate in the perinuclear region, persisting there without apparent degradation or extravasation. Drugs, small proteins, and solutes as well as  $\alpha$  particle emitting radionuclides are stably encapsulated for extended periods of time. BAPC formation at room temperature proceeds via a fusogenic process and after 48 h a range of BAPCs sizes are observed, from 50 nm to a few microns in diameter. It was previously reported that cooling BAPCs from 25 to 4 °C and then back to 25 °C eliminated their fusogenic property. In this report, biophysical techniques reveal that BAPCs undergo thermosensitive conformational transitions as a function of both time and temperature and that the properties of BAPCs vary based on the temperature of assembly. The solvent dissociation properties of BAPCs were studied as well as the contributions of specific amino acid residues to the observed conformations. The roles of the potential stabilizing forces present within the bilayer that bestow the unusual stability of the BAPCs are discussed. Ultimately this study presents revised assembly protocols for preparing BAPCs with discrete sizes and solvent-induced extravasation properties.



## 1. INTRODUCTION

Branched amphiphilic peptide capsules (BAPCs) constitute a new class of self-assembling nanodelivery vehicles, consisting of two branched, 15 and 23 amino acid polycationic amphiphilic peptide sequences that self-assemble.<sup>1</sup> The ability of the BAPCs to form bilayer-delimited spheres capable of trapping solutes is due to the unique properties of their constituent peptides. The peptide sequences bis(FLIVI)-K-K<sub>4</sub> and bis(FLIVIGSII)-K-K<sub>4</sub> (Figure 1A), present in equimolar proportions for BAPC formation, were designed to mimic diacyl phospholipids in molecular architecture, with the branch point lysine orienting the two peptide segments at  $\sim 90^\circ$  angles. The sequences reversibly transition from  $\alpha$ -helical monomers in 2,2,2-trifluoroethanol (TFE) to  $\beta$ -like structures in water where they self-assemble.

In contrast to liposomes, where the tail groups are held together primarily by hydrophobic effects and van der Waals interactions, BAPCs incorporate the additional components of hydrogen bonding and inter- and intramolecular  $\pi$ -stacking ( $\pi$ - $\pi$ ) between the phenylalanines' aromatic rings. In our earlier work published by Sukthankar et al.,<sup>2</sup> all of the biophysical studies were carried out at 25 °C. It was during the process of studying the kinetics of BAPC fusion that the process could be blocked and maintained, by storing the nascent BAPCs at 4 °C after initially forming them at 25 °C. This suggested the existence of a temperature effect that affects BAPC structure, size, and behavior. In this study, we identify



**Figure 1.** Bilayer forming peptide sequences. (A) Parent sequences. (B) Branched amphiphilic peptide amino acid replacement variants G<sup>6,6'</sup>G<sup>7,7'</sup> and A<sup>6,6'</sup>A<sup>7,7'</sup> of bis(FLIVIGSII)-K-K<sub>4</sub> peptide were designed, where the Ser-Gly residues on the 6th and 7th positions of both the branches were substituted with Gly-Gly and Ala-Ala, respectively, to generate stronger and weaker  $\beta$ -conformers of the parent sequence.

temperature-induced conformational changes in BAPCs and comment on the aspects of the peptide bilayer that contribute to these transitions.

**Received:** November 7, 2014

**Revised:** February 19, 2015

## 2. MATERIALS AND METHODS

**2.1. Peptide Synthesis.** All peptides were synthesized on a 0.1 mmol scale using solid phase peptide chemistry using Fmoc (*N*-(9-fluorenyl)methoxycarbonyl)/*tert*-butyl chemistry on an ABI Model 431 peptide synthesizer (Applied Biosystems; Foster City, CA). The Fmoc amino acids, obtained from Anaspec, Inc. (Fremont, CA), were assembled on a 4-(2,4-dimethoxyphenyl-Fmoc-aminomethyl)-phenoxyacetyl norleucyl-cross-linked ethoxylate acrylate resin<sup>3</sup> (Peptides International Inc., Louisville, KY). All amino acids were double coupled. The branch point in each sequence was introduced by incorporating *N*<sup>α,ε</sup>-di-Fmoc-L-lysine in the fifth position from the C-terminus, which upon deprotection led to the generation of the bifurcated peptide branch points. The N-terminal hydrophobic segments FLIVI, FLIVIGSII, FLIVIGGII, and FLIVIAAII were simultaneously coupled to the common hydrophilic oligo-lysine backbone.<sup>4</sup> During the synthesis of the nonaromatic sequences, the N-terminal Fmoc-L-phenylalanines were replaced with Fmoc-3-cyclohexyl-L-alanine (Sigma-Aldrich Corp., St. Louis, MO). The N-termini of the peptides were acetylated using acetic anhydride/*N,N*-diisopropylethylamine/1-hydroxybenzotriazole prior to cleavage. The peptides were cleaved from the resin using 2,2,2-trifluoroacetic acid (American Bioanalytical Inc., Natick, MA) TFA/H<sub>2</sub>O (98:2, v/v) for 90 min at room temperature (RT). The cleaved peptide products were washed three times with diethyl ether and redissolved in water prior to lyophilization. The water used throughout this study was deionized, reverse osmosis treated, and then glass distilled. The RP-HPLC purified peptides were dried *in vacuo* and characterized using a Bruker Ultraflex III matrix-assisted laser desorption/ionization time-of-flight mass spectrometer (MALDI TOF/TOF) (Bruker Daltonics, Billerica, MA) using 2,5-dihydroxybenzoic acid matrix (Sigma-Aldrich Corp., St. Louis, MO). The dried peptides were stored at RT.

**2.2. Synthesis of Cysteine-Hg-Me Variants for Electron Microscopy Analysis.** The C-terminal cysteine adducted peptides were synthesized on a 0.1 mmol scale with an additional *N*-α-Fmoc-S-*p*-methoxytrityl-L-cysteine (AnaSpec, Inc., Fremont, CA) coupled to the resin at the C-terminus prior to adding the amino acid sequence described above. The synthesis, cleavage, postcleavage processing, and characterization were performed as previously described (section 2.1). Both bis(FLIVI)-K-K<sub>4</sub>-C-CONH<sub>2</sub> and bis(FLIVIGSII)-K-K<sub>4</sub>-C-CONH<sub>2</sub> cysteine adducted peptides were solubilized in water and reacted with 1 equiv of methylmercury(II) iodide (Sigma-Aldrich Corp., St. Louis, MO) at pH 9.8 for 6 h at RT.<sup>5,6</sup> The resulting solution was reduced using vacuum evaporation and subsequently lyophilized. The percent methyl mercury incorporated was determined by measuring the concentration of free cysteine present after the coupling reaction. Unlabeled peptides of equal concentration served as the control. Samples were treated with 4 mg/mL Ellman's reagent (5,5'-dithiobis(2-nitrobenzoic acid)) (Sigma-Aldrich Corp., St. Louis, MO) at pH 8.2 in 0.1 M phosphate buffer. The absorbance values of the fully reacted sample were measured at 412 nm on a CARY 50 Bio UV/vis spectrophotometer (Varian Inc., Palo Alto, CA) using a 0.3 cm path length quartz cuvette (Starna Cells Inc., Atascadero, CA).<sup>7</sup> The concentrations of the peptides were calculated using the molar extinction coefficient ( $\epsilon$ ) of phenylalanine residues (two per sequence) at 257.5 nm (195 cm<sup>-1</sup> M<sup>-1</sup>).<sup>8,9</sup> Nonaromatic variants were quantified using the amide absorbance at 220 nm,<sup>10</sup> calibrated on the basis of the amide absorbance of their respective phenylalanine containing sequences. The yield obtained of the methyl-Hg adduct for both sequences was 77%, resulting in 23 mol % of methyl-Hg label on the water accessible surface of the bilayer.

**2.3. BAPC Formation.** The bis(FLIVI)-K-K<sub>4</sub> and bis(FLIVIGSII)-K-K<sub>4</sub> peptides were dissolved individually in neat 2,2,2-trifluoroethanol. In this solvent the peptides are helical and monomeric, thereby ensuring complete mixing when combined and remain helical upon drying, based on FT-IR spectra. The bis(FLIVI)-K-K<sub>4</sub> and bis(FLIVIGSII)-K-K<sub>4</sub> or cyclohexyl-L-alanine-LIVI and cyclohexyl-L-alanine-LIVIGSII peptide samples were then mixed in equimolar ratios to generate desired concentrations and then dried *in vacuo*. The dried peptide samples were then hydrated by the dropwise addition of

water to form the capsules. In the case of BAPC formation using the bis(FLIVIGGII)-K-K<sub>4</sub> and bis(FLIVIAAII)-K-K<sub>4</sub>, the respective peptides were used in conjunction with bis(FLIVI)-K-K<sub>4</sub> using the same mixing protocol outlined above. For the purposes of BAPC hydration at 4 and 37 °C, dried peptide samples were prepared as previously noted and hydrated with water at their respective temperatures using a heating/cooling fluid circulator (IBM Corp., Armonk, NY).

**2.4. Sample Preparation for Electron Microscopy.** The 0.23 mol equiv Me-Hg labeled capsules were prepared in a manner similar to that previously detailed above, by codissolving 0.77 mol equiv of bis(FLIVI)-K-K<sub>4</sub> and bis(FLIVIGSII)-K-K<sub>4</sub> with 0.23 mol equiv of their respective cysteine containing (77%) Me-Hg labeled variants in water, to a final concentration containing 0.1 mM for each of bis(FLIVI)-K-K<sub>4</sub> and bis(FLIVIGSII)-K-K<sub>4</sub> peptides. The dried mixture was hydrated and allowed to stand for the indicated time intervals. Carbon Type A (15–25 nm) on 300-mesh support film grids with removable Formvar (Ted Pella Inc., Redding, CA) were immersed in chloroform to release the Formvar. These were subsequently negatively (hydrophilic) glow discharged<sup>11</sup> at 5 mA for 20 s using a EMS 150 ES turbo-pumped sputter coater/carbon coater (Electron Microscopy Sciences, Hatfield, PA)—the carbon end of the grids being exposed to the plasma discharge making the carbon film hydrophilic and negatively charged, thus allowing easy spreading of aqueous suspensions. Capsule sample solutions (6  $\mu$ L) were spotted on to grids and allowed to stand for 5 min, after which excess solution was wicked off the grid with a KimWipe tissue (Kimberly-Clark Worldwide Inc., Roswell, GA) and allowed to air-dry before loading it into the FEI Tecnai F20XT field emission transmission electron microscope (FEI Co., Hillsboro, OR) with a 0.18 nm STEM HAADF resolution and a 150X–2306  $\times$  106X range of magnification.<sup>12</sup> S/TEM was carried out in the annular dark field mode with a single tilt of 23 °C. For S/TEM analysis of BAPCs prepared using bis(FLIVIGGII)-K-K<sub>4</sub> and bis(FLIVIAAII)-K-K<sub>4</sub> peptides, the peptides were studied with 0.23 mol equiv label of bis(FLIVI)-K-K<sub>4</sub>-Cys-MeHg and 0.77 mol equiv of bis(FLIVI)-K-K<sub>4</sub>.

**2.5. Circular Dichroism Experiments.** Circular dichroism (CD) experiments were conducted to analyze conformational changes in secondary structures formed by the BAPCs as well as individual peptides in water or 50% TFE/water. Data were collected on a Jasco J-815 CD spectrophotometer (Jasco Analytical Instruments, Easton, MD) using a 0.2 mm path-length jacketed cylindrical quartz cuvette (Starna Cells Inc., Atascadero, CA). Spectra were scanned from 260 to 190 nm at scan rate of 50 nm min<sup>-1</sup> with 1 nm step intervals. All experimental temperatures were maintained using a heating/cooling fluid circulator (IBM Corp.) connected to the jacketed cuvette. CD spectra were measured in "mdeg" using an average of five scans. The raw data were subtracted from blank at the appropriate temperature and smoothed using a Savitsky–Golay filter<sup>13</sup> using Spectra Analysis software provided by the manufacturer (Jasco Inc., Easton, MD). Peptide concentrations were determined using the absorbance of phenylalanine as previously described. For experiments related to the study of capsule structure at different temperatures, 1 mM each of the individual 15-mer and 23-mer peptides was used for BAPC generation, whereas for the measurement of individual peptides, peptide concentration was kept at 2 mM. The analytical parameters and total peptide concentrations for all samples measured were identical.

**2.6. Dye Encapsulation and Measurement.** BAPC (1 mM) samples were prepared by solvating the dried monomeric mixture of the constituent peptides with aqueous 2.13 mM Eosin Y (Sigma-Aldrich Corp.) and then allowed to stand for 30 min. Fluorescence of Eosin Y is strongly quenched at this concentration (Supporting Information Figure S1). Centrifugation was carried out at 14000g in an Amicon ultra-0.5 mL 30 kDa molecular weight cutoff centrifugal cellulose filters (Millipore, Billerica, MA) using a Thermo Electron Legend 14 personal microcentrifuge (Thermo Fisher Scientific Inc., Waltham, MA) to remove nonencapsulated dye. Samples were then subjected to three centrifugation cycles starting with a 5 min preincubation with 200 mM Na-TFA salt. The TFA<sup>-</sup> counterion successfully displaces Eosin Y associated with the outer capsule

surface.<sup>2</sup> For the second and third centrifugation cycles, the Eosin Y encapsulated capsules were incubated with just water prior to centrifugation. At the conclusion of the third spin, the removable-filter unit was inverted and placed in a fresh tube and spun at 2000g for 5 min to recover the remaining volume containing the washed capsules, which was then suspended in a standardized volume of water.

Fluorescence measurement of the encapsulated content was carried out by the excitation of Eosin Y at 490 nm and scanning for observed emissions from 495 to 800 nm with a CARY Eclipse fluorescence spectrophotometer (Varian Inc., Palo Alto, CA) (scan rate: 600 nm/min; PMT detector voltage: 600 V; excitation slit: 10 nm; emission slit: 10 nm) using a 0.3 cm path length quartz cuvette. Standard curves examining the concentration and temperature effects on of Eosin Y fluorescence were performed.

**2.7. Capsule Fusion Study.** 1.0 and 20.0 mM dried samples of bis(FLIVIGSII)-K-K<sub>4</sub>:bis(FLIVI)-K-K<sub>4</sub> peptide capsules were made both at either 4 or 37 °C as previously described for the 25 °C sample. Both these samples were simultaneously solvated at the respective experimental temperatures—the 1 mM sample with aqueous 2.13 mM Eosin Y and the 20.0 mM sample with water—and then allowed to stand for 30 min. All samples were subjected to the wash process described in the preceding section. At the end, both the 1.0 and 20.0 mM capsules were suspended in 4 or 37 °C water, then immediately mixed in equal volumes, and placed in a 0.3 cm quartz cuvette and scanned for observed emission from 495 to 800 nm with a scan every 5 min for the 37 °C experiments over 4 h and every 10 min for the 4 °C experiment over 8 h upon excitation at 490 nm, with a CARY Eclipse (scan rate: 600 nm/min; PMT detector voltage: 800 V; excitation slit: 5 nm; emission slit: 5 nm).

**2.8. NMR Studies.** The 1D and 2D <sup>1</sup>H–<sup>1</sup>H NMR experiments were performed at 4 and 25 °C on a 3.5 mM aqueous solution of bis(FLIVIGSII)-K-K<sub>4</sub> peptide in 10% D<sub>2</sub>O using a Varian 500 NMR System (Varian Inc., now Agilent Technologies, Palo Alto, CA) equipped with a 5 mm triple-resonance inverse detection pulse field gradient cryogenic probe operating at 499.84 MHz for <sup>1</sup>H frequency. 2D <sup>1</sup>H–<sup>1</sup>H total correlation spectroscopy (TOCSY) and NOE spectroscopy (NOESY) data were acquired in phase-sensitive (States-TPPI) mode into 4000 *t*<sub>2</sub> and 256 *t*<sub>1</sub> points with spectral width of 12 ppm in each dimension and 8 transients per increment. Spin-lock time of 80 ms at a B<sub>1</sub> field strength of 7.0 kHz was used for TOCSY experiments, and mixing times of 200, 500, and 800 ms were used for NOESY experiments. The water peak was used as a chemical shift reference. For all experiments the spectral resolution was enhanced by Lorentzian-Gaussian apodization when necessary. Data processing was done using the program VnmrJ (Varian Inc., Palo Alto, CA).

**2.9. Infrared Microspectroscopy.** All spectra were acquired using the PerkinElmer (Shelton, CT) Spectrum Spotlight IR at the Kansas State University Microbeam Molecular Spectroscopy Laboratory. Spectrum software supplied with the imaging system was used to acquire the data, and OMNIC (Thermo Scientific, Madison, WI) software was used to process the spectra. The individual bis(FLIVIGSII)-K-K<sub>4</sub>:bis(FLIVI)-K-K<sub>4</sub> peptides were dissolved in water at 25 °C and then spotted on a low-e glass infrared reflecting microscope slide (Kevley Technology, Chesterfield, OH). After evaporation a background spectrum was collected from the slide, and reflection absorption measurements of the localized peptides were taken in the 4000–800 cm<sup>-1</sup> region of the spectrum with 256 scans co-added and 25 μm image plane masking. Omnic software was then used to baseline correct the spectra prior to calculation of the second derivative and subsequent identification of peaks in the amide I band region.

#### 2.10. BAPC Temperature Shift Studies and Nomenclature.

For the temperature shift studies BAPCs were prepared using 1 mM each of the two constituent peptides. The peptides were dried together in TFE and then rehydrated with 500 μL of water at the desired temperatures to generate 1 mM BAPCs. The BAPCs were maintained at the assembly temperature for 30 min before carrying out the temperature shift analyses. The 0 min initial time point for the CD experiments refers to the instant the 30 min post hydration BAPCs

were placed in the temperature-controlled cuvettes and their spectra recorded. At 30 min, BAPC formation was complete based on TEM imaging. A shorthand nomenclature was developed to indicate the temperature shift parameters that led to the different conformational states. They are represented as follows: “*x*-*y*-*z* (*T* °C) BAPCs”, where *x* = temperature of BAPC formation; *y*, *z* = transition temperatures in that order, and *T* = temperature at which BAPCs were studied. For instance, in the case of 25-4-25 (25 °C) BAPCs, the capsules were prepared at 25 °C for 30 min and then dropped to 4 °C for 60 min before being brought back to 25 °C and then measured at 25 °C.

### 3. RESULTS AND DISCUSSION

**3.1. BAPCs Undergo Temperature-Based Conformation Changes.** In a previously reported experiment<sup>2</sup> the self-quenching fluorescence property of Eosin Y was exploited to analyze the fusion kinetics of peptide capsules formed at 25 °C. Nascent BAPCs encapsulating Eosin Y were allowed to fuse with a 20-fold excess of nascent BAPCs containing just water. Fusion of the dye containing capsules with the water containing ones diluted the dye resulting in an increase in fluorescence. As the fusion process progressed, the increasing intensities of the fluorescence emissions were recorded. As part of the experimental design, an aliquot of the sample was cooled to 4 °C to see if fusion could be arrested. Upon returning the sample to 25 °C, 6 h later, fusion did not occur, even when the temperature was raised to 85 °C. The fluorescence intensity remained identical to that of the initial time point.

Another feature of the BAPCs is their ability to transition from a β-like conformation in water back to an α-like helical conformation in 50% TFE/H<sub>2</sub>O.<sup>1</sup> Under these conditions the BAPCs disassemble and release their contents, thus permitting quantification of the encapsulated solutes. As illustrated in Figure 2, BAPCs encapsulating 2.13 mM Eosin Y at 25 °C

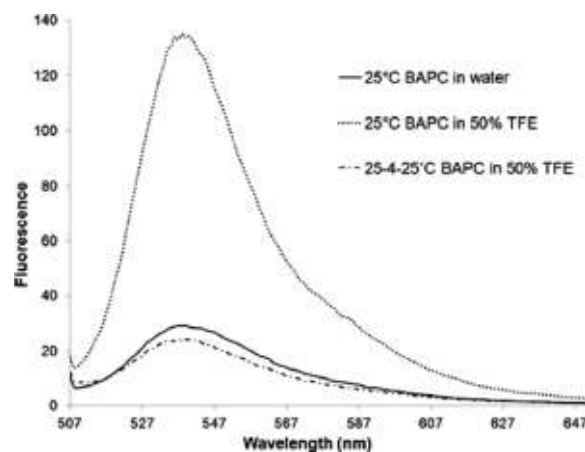


**Figure 2.** Representative fluorescence scans of 25 °C and 25-4-25 °C 2 mM BAPCs in water and 50% TFE, encapsulating 2.13 mM Eosin Y. BAPCs formed at 25 °C rupture in 50% TFE, releasing the autoquenching dye Eosin Y, resulting in increased fluorescence; however, BAPCs prepared at 25 °C, when cooled to 4 °C for 30 min and then brought back to 25 °C, do not rupture in 50% TFE. All measurements were carried at 25 °C.

readily release the dye in 50% TFE/H<sub>2</sub>O, resulting in the observed increase of fluorescence intensity. We observed an identical response with BAPCs prepared at 25 °C that are then cooled and held at 4 °C. However, if the 25 °C BAPCs cooled to 4 °C capsules were returned to 25 °C, addition of TFE did not give the expected increase in fluorescence. Transitioning



the cooled sample back to 25 °C appears to trigger a temperature-based alteration that confers resistance to disruption in 50% TFE/H<sub>2</sub>O.

CD spectra were recorded for the 25-4 (4 °C), 25-25 (25 °C), and 25-4-25 (25 °C) BAPCs. The 25-4 (4 °C) BAPCs appear to be predominantly random coil while the 25-25 (25 °C) BAPCs appear to be a mixture of random coil and  $\beta$ -like structures. Immediately upon returning the 25-4 °C BAPCs to 25 °C their spectrum resembles that seen for the 25-25 (25 °C) BAPCs and remains unchanged 30 and 60 min later (Figure 3).

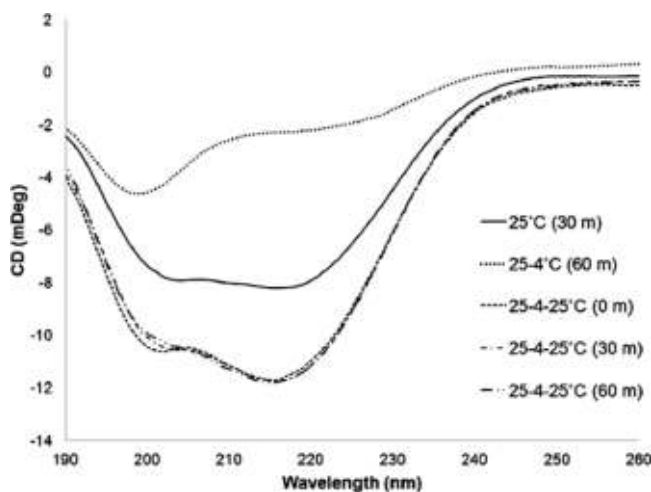


**Figure 3.** CD scans of 25-4-25 (25 °C) BAPCs. 1 mM BAPCs were made at 25 °C and allowed to stand for 30 min [25 (25 °C) BAPCs] after which they were subjected to a 4 °C cycle for 60 min [25-4 (4 °C) BAPCs] before being brought back to 25 °C [25-4-25 (25 °C) BAPCs]. Spectra were recorded at 0, 30, and 60 min upon warming to 25 °C.

These results suggest that all BAPCs at 25 °C display mixed conformations that include both  $\beta$ -like and random structures. However, similar in appearance the spectra are for the 25-4-25 (25 °C) BAPCs and the 25-25 (25 °C) sample; they must be different based on the 25-4-25 (25 °C) BAPCs' newly acquired resistance to disassembly in 50% TFE/H<sub>2</sub>O. We refer to the "25-4-25 (25 °C)" conformation as "locked".

Follow-on experiments were performed to better understand this new behavior.

**3.2. BAPC Structural Transitions as a Function of Temperature and Time.** CD was used to document the secondary structural changes that occurred over time for BAPCs formed initially at 25 °C and then either kept at 25 °C or transitioned to either 4 or 37 °C. In this study the CD spectra were recorded at the final transition temperature at 0, 30 min, and 24 h (Figure 4). As a control experiment the release of encapsulated Eosin Y was monitored for each condition. No dye release occurred during the entire experiment, indicating that the BAPCs retained their structural integrity throughout the experiment. At the initial time point (top panel), the 25-4 (4 °C) BAPCs revealed a profile with both 198 and 218 nm minima present. At 30 min (middle panel) the negative band at 198 nm was unchanged while the negative band at 218 nm was more positive. At 24 h, the intensity of the 198 nm band became considerably more negative while the 218 nm became slightly more negative. The observed temperature transition led to a shift in the spectral minima, suggesting a transition from a mixture of  $\beta$ -like and

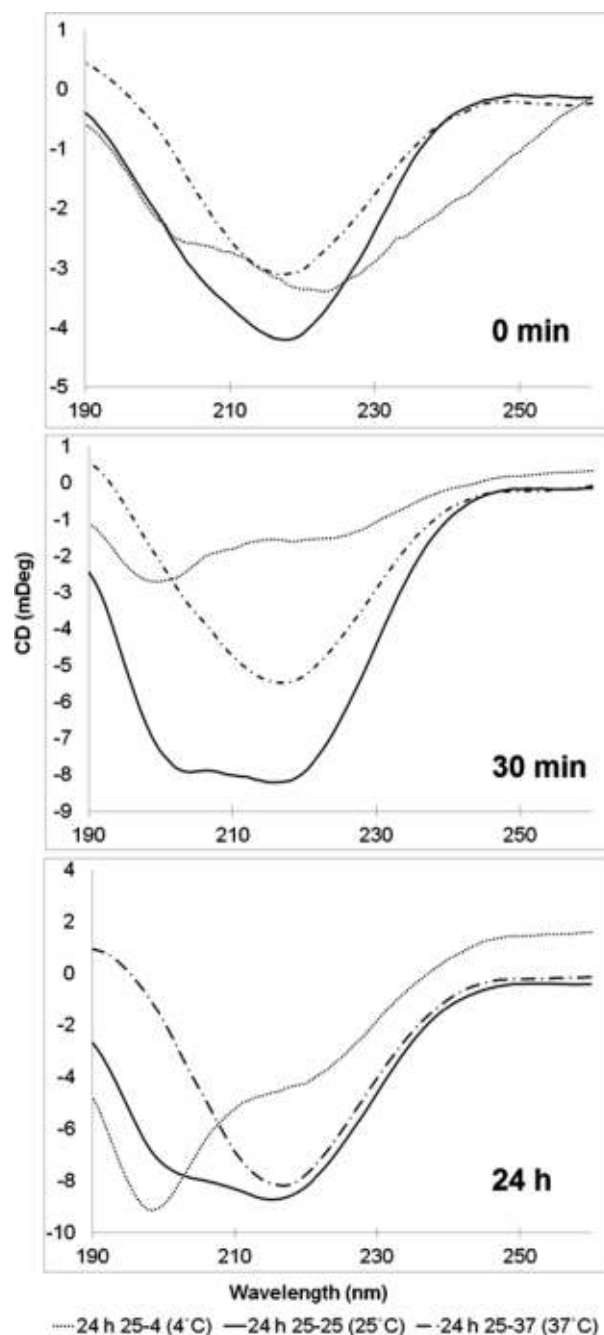


**Figure 4.** CD Spectra of BAPC conformers at different temperatures. 1 mM BAPCs were prepared at 25 °C and then taken to, or retained at, 4, 25, and 37 °C. CD spectra shown here were measured at initial time point post-transition (top panel), 30 min (middle panel), and at 24 h (bottom panel).

random coil to predominantly random coil conformers. These conformational transitions are quite different compared to those observed for the "25-4-25 (25 °C)" sample (Figure 3). The BAPCs transitioned to and held at 4 °C display more random coil. There was also a greater time dependence for the refolding of the peptides that was not seen with the 25-4-25 (25 °C) sample. At time = 0, the 25 °C spectrum indicated initially a  $\beta$ -like conformation; however, by 30 min minima at both 218 and 198 nm that were matched with respect to the negative deflection were present. At 30 min uniform 20–30 nm diameter BAPCs are typically observed which go on to fuse

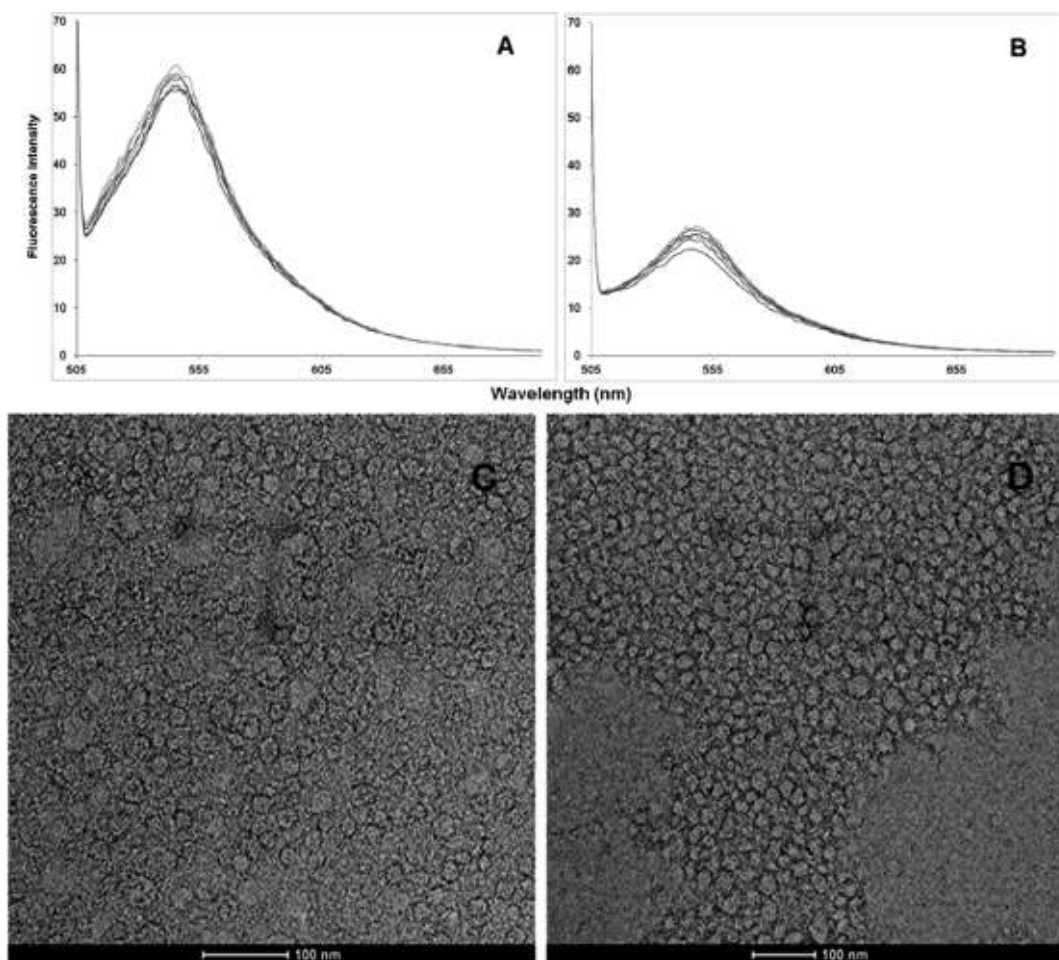


**Figure 5.** BAPC assembly and encapsulation at 4 and 37 °C. All BAPCs were prepared at their respective experimental temperatures, which were maintained during the course of the experiment. (A) BAPC fusion at 4 °C and (B) BAPC fusion at 37 °C. Salt washed Eosin Y encapsulating BAPCs hydrated at 4 and 37 °C were mixed with water-filled BAPCs in the ratio of 1:20 at 4 and 37 °C, respectively. Initial and hourly scans over 6 h experimental time scales have been shown for the sake of clarity. TEM images of BAPCs: (C) BAPCs hydrated at 4 °C and (D) BAPCs hydrated at 37 °C. 0.1 mM BAPCs with 23% Hg label on bis(FLIVI)-K-K<sub>4</sub> were hydrated and incubated at 4 and 37 °C, respectively, for 30 min. Samples were spotted on grids and stained with 2% uranyl acetate prior to imaging. Scale bar represents 100 nm.

after 60 min.<sup>2</sup> The 24 h sample showed a slightly deeper minimum at 218 over the 198 nm one. We have previously reported that 25 °C BAPCs allowed to stand for 24 h fuse into a heterogeneous mixture of capsules that range in size from about 50 to 500 nm in diameter. By 48 h they attain sizes in the micron range.<sup>2</sup> As they increase in size, the strain due to curvature lessens. The spectrum at 24 h reflects a slight shift to a more ordered structure; however, there is still a major percentage of random structure remaining. Comparing the CD profiles of the 25 (25 °C) sample with the 25-4-25 (25 °C) sample (Figure 3), the general shapes of the profiles have a similar double minima appearance; however, the minima are slightly different, and the 25 °C sample has less of a time dependence for refolding.

For the last part of this study nascent BAPCs were prepared at 25 °C and then heated to 37 °C. This temperature shift resulted in the loss of the 198 nm band observed at 25 °C, with retention of the 218 nm minima although at a lower negative value. The CD spectra were virtually identical with regard to the position of the minima over the course of the reaction; however, the negative intensity increased at each time point. Comparing all three temperature profiles, the 25-4 (4 °C) appeared to be the most disordered with 25 (25 °C) occupying

an intermediate state with both random and  $\beta$ -structures with 25-37 (37 °C) showing the greatest  $\beta$ -like structure. The lower temperatures spectra were distinctive in that no positive signals were observed in the three samples. The 218 nm minimum is generally ascribed to  $\beta$ -structure; however, there is always a strong maximum band around 198 nm associated with it. Since the 198 nm maximum was never observed at 4 and 25 °C and there was still a relatively strong negative 198 nm, we propose that random coil is predominating in these samples. Incubation at 37 °C generated a single negative minimum at 218 nm and a small positive band at 198 nm, suggesting that this condition leads a higher percentage of  $\beta$ -structure.

**3.3. BAPC Properties Alter Based on Assembly Temperature.** In the previous experiment we examined nascent BAPCs that were prepared and then transitioned from 25 °C. Here we examined whether the peptides incubated at just 4 and 37 °C still supported assembly and were able to fuse and disassemble in the presence of 50% TFE in water. For these experiments we looked at the encapsulation and release of the dye Eosin Y. As before,<sup>2</sup> bis(FLIVI)-K-K<sub>4</sub> and bis(FLIVIGSII)-K-K<sub>4</sub> were mixed in 100% TFE, dried, and then rehydrated with in the presence of 2.13 mM Eosin Y in water at 4 and 37 °C, respectively. After washing to remove surface

associated dye, the extent of dye encapsulation was measured. BAPCs were maintained at the two different assembly temperatures throughout the course of these experiments. These results indicate that BAPCs can assemble at these different temperatures even though they show different secondary structures. We subsequently studied the 4 and 37 °C nascent BAPCs for fusion (Figure 5A,B). BAPCs (1 mM) encapsulating 2.13 mM Eosin Y at 4 or 37 °C were mixed with 20 mM water-filled BAPCs at 4 and 37 °C, respectively. Temperatures were maintained throughout the process of hydration, washing, assembly, and fusion steps. Eosin Y emission scans were carried out every 5 min for the 37 °C experiments over 4 h and every 10 min for 4 °C experiments for 8 h. No significant change in the fluorescence intensity was seen at either temperature indicating that fusion had not occurred when the nascent BAPCs were formed at 4 and 37 °C. TEM images were generated for both of the 4 and 37 °C samples. Representative images of the BAPCs are shown in Figure 5C (4 °C) and Figure 5D (37 °C). For both the 4 and 37 °C BAPCs formed uniform 20–30 nm diameter capsules at 30 min similar to 25 °C BAPCs at 30 min.<sup>2</sup> If temperature-induced kinetic factors were playing a role in BAPC fusion, larger BAPCs should have been observed for the 37 °C experiment, as opposed to the 4 °C ones. However, no such distinction was seen. Looking at the dye intensities for the three temperatures, the 4 °C BAPCs encapsulated more Eosin Y as compared to the 37 °C BAPCs, with 25 °C being intermediate (Figure 6) even when the dye intensities were corrected for

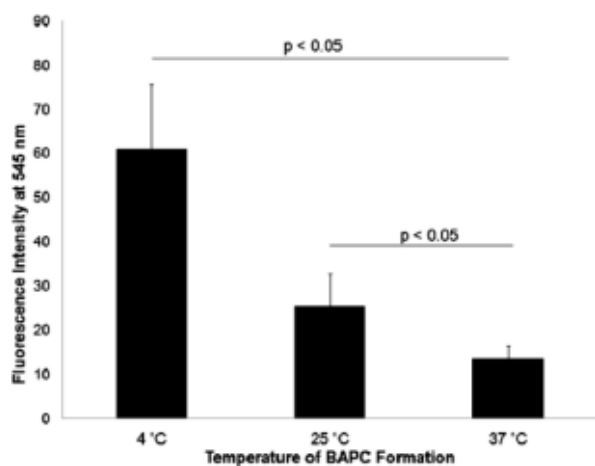


**Figure 6.** Encapsulation of Eosin Y. 1 mM BAPCs containing 2.13 mM Eosin Y were prepared at 4, 25, and 37 °C as previously detailed. The highest encapsulation was seen in the case of BAPCs prepared at 4 °C. Error bars represent SEM with  $n \geq 3$ .

temperature effects (Figure S2). Volume being a cubic function of measurement, a small increase in diameter in a spherical system would result in a much larger increase in its ability for encapsulation. Calculations based on the eosin encapsulation data suggest that BAPCs prepared at 4 °C would either be >4-fold more abundant than those prepared at 37 °C or that the diameter of the 4 °C BAPCs would be 3× larger than those made at 37 °C. Since the TEM image measurements were not able to discern any significant difference in their sizes, it is likely that the increase in encapsulation can be attributed to a higher efficiency of BAPC formation at 4 °C vis-à-vis 25 and 37 °C. It is probable that a higher propensity toward aggregation at 37 °C might result in lower efficiency of BAPC assembly at that

temperature. These results indicate that stable and homogeneously sized BAPCs will form when prepared at 4 or 37 °C conditions where more homogeneous conformations (mostly random or mostly beta secondary structures) occur and that these conformers do not require fusion to relieve strain due to curvature.

**3.4. Contribution of the Constituent Peptides to BAPC Conformation.** BAPCs are composed of peptides that reversibly transition from  $\alpha$ -helices in TFE to  $\beta$ -like structures in water.<sup>1</sup> Sequence elements that contribute to the formation of the  $\beta$ -like structure are not fully understood. Intrinsic  $\beta$ -sheet propensities for certain amino acids have been implicated; however, there are no well-defined rules predicting  $\beta$ -sheet formation.<sup>14</sup> CD experiments were performed on the individual BAPC-forming peptide segments to elucidate the structural elements that contribute to the observed thermally induced conformation changes. It should be noted that the individual peptides bis(FLIVI)-K-K<sub>4</sub> and bis(FLIVIGSII)-K-K<sub>4</sub> will not form capsules individually. Both the longer and shorter sequences must be present for capsule formation. Under the conditions tested, the peptides could form associations but not capsules. Initially the individual peptides were dissolved in 25 °C water to induce  $\beta$ -structure and then dried. The infrared spectra of both the bis(FLIVIGSII)-K-K<sub>4</sub> and bis(FLIVI)-K-K<sub>4</sub> peptides showed a variety of secondary structure contributions to the amide I band. In Figure S4, note the prevalence of unordered structure due to the strong band at 1640 cm<sup>-1</sup> for both peptides. The small contribution at 1681 cm<sup>-1</sup> for the bis(FLIVIGSII)-K-K<sub>4</sub> points to the presence of a  $\beta$ -hairpin in the dried sample.<sup>15</sup>

Experiments carried out in other polypeptide model systems have indicated that a glycine–serine dyad can contribute to the stabilization of  $\beta$ -turn motifs.<sup>16,17</sup> In order to study the possible contribution of this dipeptide to the mutable conformations the bis(FLIVIGSII)-K-K<sub>4</sub> peptide, two substituted sequences were prepared: bis(FLIVIGGII)-K-K<sub>4</sub>, a branched amphiphilic peptide that should exhibit a tighter  $\beta$ -turn, and bis(FLIVIAAII)-K-K<sub>4</sub>, a peptide that should exhibit a weaker  $\beta$ -turn (sequences shown in Figure 1B).<sup>18,19</sup> The temperature effects on secondary structure of peptides alone were analyzed by CD on bis(FLIVI)-K-K<sub>4</sub>, bis(FLIVIGSII)-K-K<sub>4</sub>, and the new sequences. All samples were dissolved and then analyzed at 4, 25, and 37 °C. The spectra in Figure 7A for the bis(FLIVI)-K-K<sub>4</sub> sequence showed the least amount of structural variability across all temperatures and also showed the highest degree of random coil. This is expected since this sequence is composed of just 15 residues and does not contain the gly-ser dyad. The contribution of temperature to  $\beta$ -structure in the branched nine residue sequences is evident in Figure 7B–D where increases in  $\beta$ -like character were observed in the samples measured at both 25 and 37 °C. In Figure 7B the bis(FLIVIGSII)-K-K<sub>4</sub> peptide displays random structure at 4 °C but  $\beta$ -like structure at the higher temperatures. This result is consistent with the CDs recorded for the BAPCs at 4 °C where the overall structure was random (Figure 3A). The 25 °C BAPC CD spectra are consistent with a mixture of the bis(FLIVI)-K-K<sub>4</sub> (random) and bis(FLIVIGSII)-K-K<sub>4</sub> ( $\beta$ -like structure) (Figure 3B). At 37 °C the BAPC CD showed more  $\beta$ -like structure than a composite of the two individual CDs (Figure 3C). This apparent anomaly might suggest some type of cooperative or induced effect, where at higher temperatures the smaller peptide can transition to a  $\beta$ -like structure upon interacting with the larger  $\beta$ -like structured peptides.



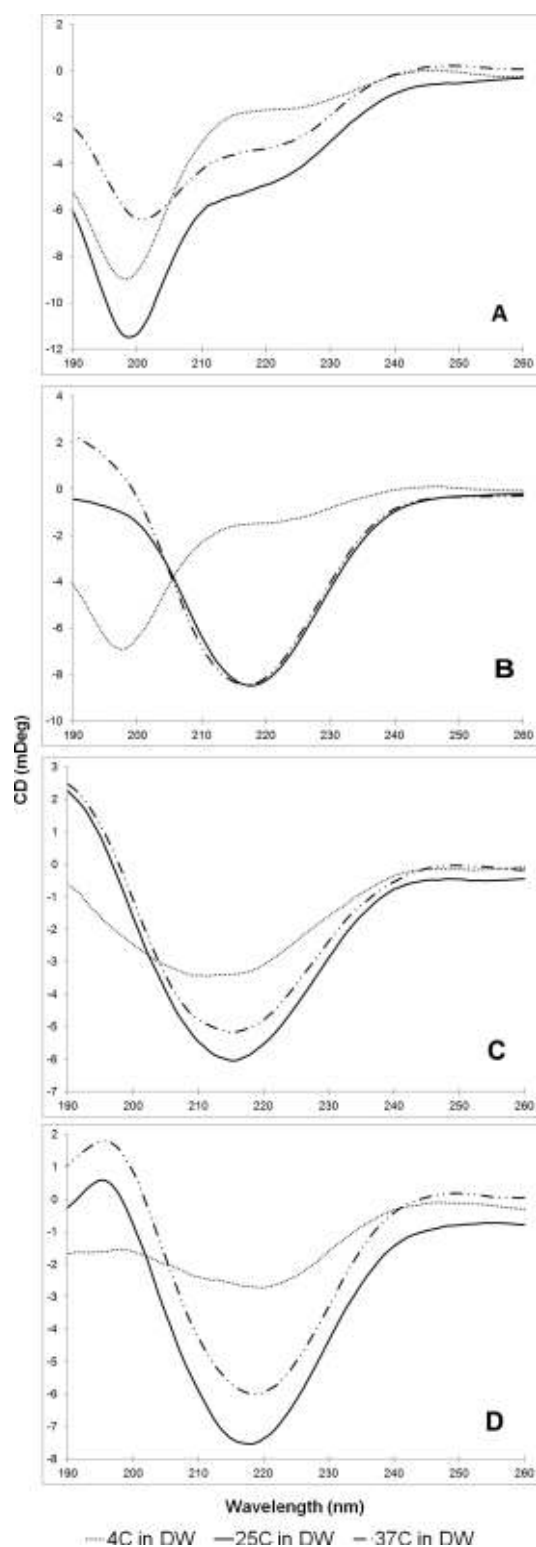


**Figure 7.** Circular dichroism spectra of branched amphiphilic peptides at 4, 25, and 37 °C. 2 mM concentrations of (A) bis(FLIVI)-K-K<sub>4</sub>, (B) bis(FLIVIGSII)-K-K<sub>4</sub>, (C) bis(FLIVIAAI)-K-K<sub>4</sub>, and (D) bis(FLIVIGGII)-K-K<sub>4</sub> in water at 4, 25, and 37 °C.

The bis(FLIVIAAI)-K-K<sub>4</sub> sequence (Figure 7C) showed  $\beta$ -like character at 25 and 37 °C, but with less negative minima. This is indicative of the fact that although the ser-gly residues in the FLIVIGSII sequence contribute to the formation of the  $\beta$ -conformers, there are undoubtedly other residual, steric, and

electrostatic forces within these branched sequences that enable the ala-ala variant to adopt a  $\beta$ -like structure. The bis(FLIVIAAI)-K-K<sub>4</sub> sequence does however show the least amount of secondary structural variation between 25 and 37 °C, suggesting the temperature-based variations within this range rely on the presence of turn forming residues in the 6th and 7th positions.

The bis(FLIVIGGII)-K-K<sub>4</sub> variant (Figure 7D) at 25 and 37 °C displayed the greatest negative minima at 218 nm as well as the best defined positive maxima around 195 nm. Together these CD bands indicate that the gly-gly containing peptide shows the greatest degree of  $\beta$ -like character.<sup>20</sup>

The transition to 4 °C brings about a reduction in  $\beta$ -like structure in all studied sequences. This suggests that factors other than the turn forming residues contribute to this transition. If the ser-gly turn residues exclusively dictated the  $\beta$ -character, then the weaker  $\beta$ -forming ala-ala variant would not have demonstrated a loss of  $\beta$ -conformation at 4 °C, and alternately the stronger gly-gly variant should have retained its  $\beta$ -structure at all studied temperatures. It is only the parent sequence bis(FLIVIGSII)-K-K<sub>4</sub> that shows a complete transition from a classic  $\beta$  to a coil-like structure. To confirm the absence of structure for the parent sequence at this temperature, both TOCSY and NOESY NMR experiments were performed. Analysis of 2D <sup>1</sup>H-<sup>1</sup>H NOESY NMR experiments conducted on a sample of aqueous solution of bis(FLIVIGSII)-K-K<sub>4</sub> in 10% D<sub>2</sub>O at 4 °C revealed the absence of the characteristic NOE cross-peaks expected for secondary structure elements (Figure S5), also indicating the lack of secondary structure for the peptide monomers at 4 °C.

The conformational transition of bis(FLIVIGSII)-K-K<sub>4</sub> from a mixed conformation at 25 °C to a more random structure at 4 °C appears to be driven by the presence of the ser-gly residues at the 6,6' and the 7,7' positions. There also appears to be a synergistic association between the bis(FLIVIGSII)-K-K<sub>4</sub> and bis(FLIVI)-K-K<sub>4</sub> sequences that enables the BAPCs to seamlessly transition from one state to another. This transformation into a predominantly homogeneous random coil conformation at low temperatures might account for the BAPC's inability to fuse at 4 °C, suggesting that it is the conformational characteristics of the bis(FLIVIGSII)-K-K<sub>4</sub> that is one of the driving forces behind BAPC fusion.

**3.5. BAPC Stabilizing Interactions.** In earlier studies we observed a much greater thermal stability for the BAPCs when compared to diacylphospholipid vesicles.<sup>1</sup> The process of molecular self-assembly for biomaterials is typically mediated by numerous weak noncovalent yet specific intra- and intermolecular interactions such as hydrogen bonding and van der Waals forces. The structural properties of the building blocks generally direct the architecture and properties of the supermolecular structure.<sup>21</sup> Differential scanning calorimetry experiments previously performed on BAPCs identified the BAPCs as stable constructs capable of maintaining their integrity to at least 95 °C, the highest temperature tested.<sup>1</sup> This coupled with the fact that BAPCs were able to stably encapsulate the  $\alpha$ -particle-emitting radionuclide <sup>225</sup>Ac for extended periods of time, without any measurable release after the recoil of the daughter radionuclides, suggested factors other than hydrogen bonding and hydrophobic interactions could be contributing to their robust properties.<sup>22</sup> In addition to their ability to form hydrogen bonds, another characteristic of the BAPCs is the presence of numerous aromatic phenylalanines (~4000 per bilayer) located at the leaflet

interface, well positioned to promote intermolecular  $\pi$ - $\pi$  stacking interactions.<sup>1,2</sup> Aromatic interactions are known to contribute to the structural stabilization of proteins and confer them with thermophilic and thermostable properties by imparting rigidity and directing their packing geometry.<sup>23</sup> A pair of aromatic interactions can contribute between  $-0.6$  and  $-1.3$  kcal/mol to the stability of the protein.<sup>24</sup> We speculate that the presence and close proximity of these aromatic residues play a crucial role in imparting order and directionality to the self-assembly process by contributing to the free energy of formation. To test this hypothesis, the phenylalanines in the bis(FLIVIGSII)-K-K<sub>4</sub> and bis(FLIVI)-K-K<sub>4</sub> peptides were replaced with cyclohexyl-L-alanine (Cha), a nonencoded structural analogue acid devoid of aromatic character. The Cha-containing BAPCs were prepared at 25 °C for 30 min, after which they were taken to 4 °C for 60 min before being brought back to 25 °C. The cyclohexylalanine peptide variants formed BAPCs, which was confirmed by their ability to encapsulate Eosin Y and then release the dye when placed in 50% TFE/50% H<sub>2</sub>O. The CD spectra for these nonaromatic BAPCs (Figure 8) showed strong  $\beta$ -like character throughout

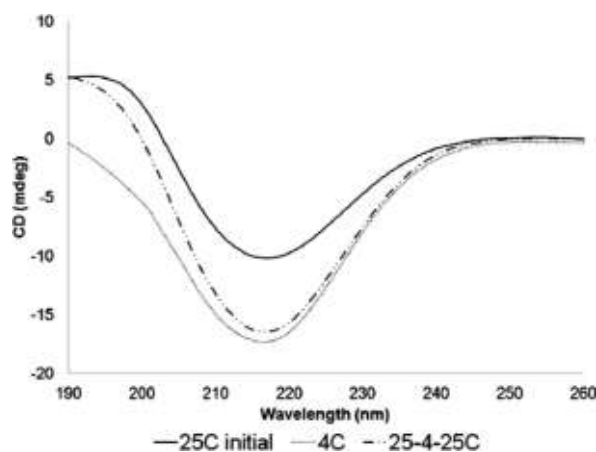


**Figure 8.** CD spectra of 25-4-25 °C Cha-BAPCs. 1 mM Cha-BAPCs were made at 25 °C and allowed to stand for 30 min, after which they were cooled to 4 °C for 60 min before returning them to 25 °C.

all of the temperature transitions tested. While the presence of the positive maxima is lost when taken to and held at 4 °C, it returns when brought back to 25 °C. Unlike the BAPCs containing phenylalanines, we do not see the presence of double minima at 25 °C, nor do we see the generation of the random coil conformation at 4 °C (Figure 3), indicating that the presence of the aromatic phenylalanines also contributes to BAPC conformations.

Fusion experiments (Figure 9) were performed using 1 part Eosin Y containing Cha-BAPCs mixed with 20 parts of just water containing BAPCs, in an analogous experiment to that previously described in Figure 5. In this experiment a completely new behavior was observed. This is the first situation where the BAPCs in addition to not fusing, appeared to be decreasing in size over time. Up until 60 min the fluorescence intensity of the Eosin Y decreased. This could only occur if the concentration of the dye increased with the loss of the noncompressible water as the Cha-BAPCs decreased in size. The structural rearrangements that lead to this change are unknown at this time. As a control in the absence of the aromatic residues, the 25-4-25 (25 °C) Cha-BAPCs do not lock-

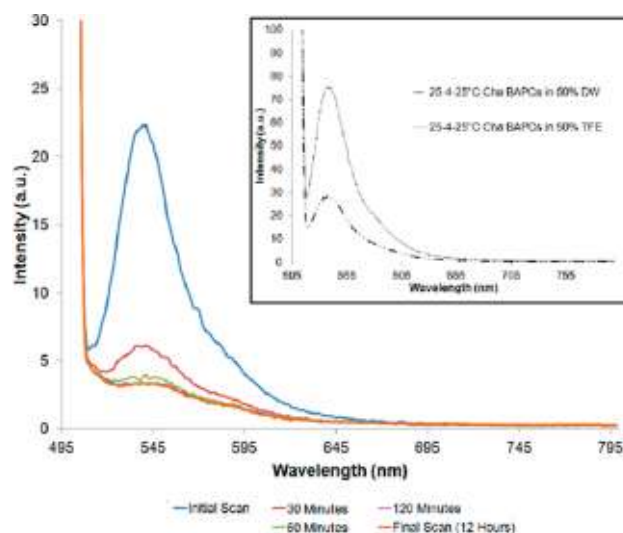


**Figure 9.** Fusion studies of Cha-BAPC. The fusion experiment was prepared at room temperature as discussed previously but with Cha-BAPCs. Scans were repeated every 30 min with the temperature maintained at 25 °C during the entirety of scans. By 120 min into scan, intensity of fluorescence was the same as seen in the final scan. Inset: Cha-BAPC rupture in TFE. All BAPCs were prepared with the Cha variant at room temperature. The BAPCs were then cooled to 4 °C and brought back to 25 °C where they were scanned. The sample was diluted in 50% water or 50% TFE.

in as seen with the parent 25-4-25 (25 °C) (Figure 9 inset) and release their contents when exposed to a 50% TFE water solution. These results indicate that the chemical character of the residues at the bilayer leaflet interface influence the behavior of the BAPCs.

#### 4. CONCLUSION

BAPCs constitute a novel class of peptide bilayer forming nanocarriers that are capable of traversing cellular membranes and persisting inside the cell with no apparent cytotoxicity.<sup>22</sup> At times during the early phase of the fusion studies on Eosin Y loaded BAPCs (conducted at RT) yielded inconsistent results—working one day but not another. It was not until strict temperature control was maintained throughout the experiments that the profiles and kinetics become fully reproducible. This observation stimulated the design of experiments to catalog and explain the anomalous temperature-sensitive characteristics of these capsules. It is evident that the BAPCs and their constituent peptides display a great degree of conformational variation over a relatively small temperature range, with the temperature of BAPC formation dictating their final biophysical properties. When mature BAPCs (25 °C for >2 h) were used for the temperature structure transition studies, no alterations in the CD spectra were seen at any of the temperatures tested. By 2 h, the mature 25 °C BAPCs had undergone fusion, forming capsules with diameters ranging from 20 to 500 nm, thereby reducing strain due to curvature.<sup>2</sup> This result indicated that only nascent BAPCs have the ability to modify their conformations.

In Figure 10 the four different temperature-dependent states of the BAPCs are illustrated. They all appear to adopt conformations that were not reversible under the conditions tested. We now know that uniform and stable 20–30 nm sized BAPCs can be formed directly by assembling them at 4 or 37 °C. This size has been reported to be ideal for cell and tissue



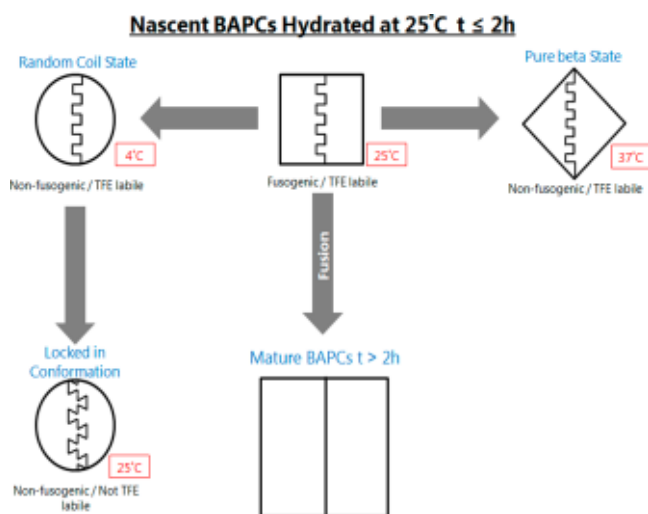


**Figure 10.** Various fates of the 25 °C incubated BAPCs. All states shown are irreversible. BAPCs hydrated at 4 and 37 °C form uniform 20–30 nm diameter nonfusogenic capsules that are disrupted with TFE.

uptake.<sup>25–27</sup> It is evident that there exists an interplay between the bis(FLIVIGSII)-K-K<sub>4</sub> and bis(FLIVI)-K-K<sub>4</sub> peptides that constitute the BAPCs. Only together do the BAPCs form. The interactions involve different attractive forces and packing interactions that must realign as the peptides sample different conformations. Initially the smaller unstructured bis(FLIVI)-K-K<sub>4</sub> peptides most likely help compensate for curvature strain as previously hypothesized,<sup>1</sup> by filling voids and associating with the bis(FLIVIGSII)-K-K<sub>4</sub> peptides that exist as both random coil and  $\beta$ -like conformation as a function of temperature. We speculate that the process of assembling these mixed conformers results in a metastable high-energy state. These nascent 25 °C BAPCs then undergo fusion to reach a lower energy state that involves a conformational shift that is enriched in  $\beta$ -conformers.

We speculate that when nascent 25 °C BAPCs are taken to 4 °C, the bis(FLIVIGSII)-K-K<sub>4</sub> adopts a random coil structure resulting in BAPCs with homogeneously random coil peptides that interact more freely than before. With the bis(FLIVIGSII)-K-K<sub>4</sub> wanting to return to  $\beta$ -like structure when brought back to 25 °C, the homogeneous interaction at 4 °C leads to entanglement at 25 °C, thus resulting in 25–4–25 °C “locked-in” BAPCs that cannot be dissociated by TFE. BAPCs made at 25 °C when taken to either 4 or 37 °C, stop fusing and irreversibly change their conformation, indicating that both 4 and 37 °C seem to define new minimum-energy states.

The studies on the bis(FLIVIGGII)-K-K<sub>4</sub> and bis(FLIVIAAII)-K-K<sub>4</sub> replacements showed that removing the gly-ser dyad led to more structured conformers. Preliminary results indicated that BAPCs formed using bis(FLIVIGGII)-K-K<sub>4</sub> (strong  $\beta$ ) showed lower encapsulation compared to BAPCs formed using bis(FLIVIAAII)-K-K<sub>4</sub> (weak  $\beta$ ) (Figure S3). This coupled with the fact that BAPCs formed at 4 °C show greater encapsulation compared to those formed at 25 and 37 °C seems to suggest that the conformational state of the bis(FLIVIGSII)-K-K<sub>4</sub> sequence at a given temperature dictates the nature and efficiency of BAPC assembly and packing. It can be assumed that the larger bis(FLIVIGSII)-K-K<sub>4</sub> sequence is vital to regulating BAPC behavior. The contribution of  $\pi$ - $\pi$  interactions in defining BAPC behavior and conformation was

assessed by our studies on BAPCs, where cyclohexyl-L-alanine, a nonaromatic analogue, was substituted for phenylalanine in both sequences. These Cha-BAPCs adopt a strong  $\beta$ -like conformation throughout the process of temperature transitions. And while some variation in the character of the  $\beta$ -like structure as a function of temperature is evident from the CD spectra studies, the ability of this nonaromatic BAPC construct to form a random coil structure is lost. This seems to suggest that the nature of aromatic  $\pi$ - $\pi$  interactions within the BAPC bilayer interface plays a vital role in stabilizing the random coil conformation of the capsules at lower temperatures. It is likely that this process proceeds via an alteration in packing geometry of the bilayer of the aromatic versus the nonaromatic BAPC variant. As is to be expected, the Cha-BAPCs—devoid of the metastable intermediate at 25 °C—did not fuse, nor were the 25–4–25 (25 °C) Cha-BAPCs resistant to rupture with TFE.

Here, we have described a few of the unique conformational variants that BAPCs can adopt and how those conformations dictate whether they will undergo fusion or retain their 20–30 nm diameters. These conformers also are responsible for higher efficiencies of encapsulation and greater stability. We have also indicated that a vital key to modulating BAPCs stability lies in altering the conformational traits of the bis(FLIVIGSII)-K-K<sub>4</sub> sequence. We posit that it would be possible to selectively destabilize BAPCs by incorporating strategically engineered variants of the FLIVIGSII sequence in appropriate ratios with the original BAPCs. We are currently in the process of studying the numerous BAPC conformations described here that likely exhibit cellular and/or biophysical characteristics distinct from the 25 °C BAPCs. Furthermore, to obtain a more comprehensive understanding of the factors dictating BAPC behavior, the contributions of the aromatic residues at the interface of the bilayer to BAPC stability, the  $\pi$ - $\pi$  interactions therein, and the nature of the packing geometry of the BAPC bilayer need further investigation.

## ■ ASSOCIATED CONTENT

### 📄 Supporting Information

Figures S1–S5. This material is available free of charge via the Internet at <http://pubs.acs.org>.

## ■ AUTHOR INFORMATION

### Corresponding Author

\*E-mail: [jtomich@ksu.edu](mailto:jtomich@ksu.edu) (J.M.T.).

### Notes

The authors declare no competing financial interest.

## ■ ACKNOWLEDGMENTS

Partial support for this project was provided by PHS-NIH grants GM 074096, the Terry Johnson Cancer Center Innovation award (to J.M.T), the Terry Johnson Cancer Center for summer support (to P.S.), and the Terry Johnson Cancer Center undergraduate research award (to S.W.). This is publication 15-106-J from the Kansas Agricultural Experiment Station. We thank Dr. David Moore and Dr. Prem Thapa at the University of Kansas Microscopy and Analytical Imaging Laboratory for electron microscopy studies. We thank Zhiguang Jia for the TOC figure and Dr. Jianhan Chen at the Department of Biochemistry and Molecular Biophysics at Kansas State University for his critique of the manuscript.

## ABBREVIATIONS

BAPCs, branched amphiphilic peptide capsules; TFE, 2,2,2-trifluoroethanol; CD, circular dichroism spectroscopy; S/TEM, scanning transmission electron microscopy; EM, electron microscopy; DLS, differential scanning calorimetry; NMR, nuclear magnetic resonance; TOCSY, total correlation spectroscopy; NOESY, nuclear Overhauser effect spectroscopy.

## REFERENCES

- (1) Gudlur, S.; Sukthankar, P.; Gao, J.; Avila, L. A.; Hiromasa, Y.; Chen, J.; Iwamoto, T.; Tomich, J. M. Peptide nanovesicles formed by the self-assembly of branched amphiphilic peptides. *PLoS One* **2012**, *7*, e45374.
- (2) Sukthankar, P.; Gudlur, S.; Avila, L. A.; Whitaker, S. K.; Katz, B. B.; Hiromasa, Y.; Gao, J.; Thapa, P.; Moore, D.; Iwamoto, T.; Chen, J.; Tomich, J. M. Branched oligopeptides form nanocapsules with lipid vesicle characteristics. *Langmuir* **2013**, *29* (47), 14648–14654.
- (3) Kempe, M.; Barany, G. CLEAR: A novel family of highly cross-linked polymeric supports for solid phase synthesis. *J. Am. Chem. Soc.* **1996**, *118*, 7083–7093.
- (4) Iwamoto, T.; Grove, A.; Montal, M. O.; Montal, M.; Tomich, J. M. Chemical synthesis and characterization of peptides and oligomeric proteins designed to form transmembrane ion channels. *Int. J. Pept. Protein Res.* **1994**, *43*, 597–607.
- (5) Gruen, L. C. Stoichiometry of the reaction between methylmercury (II) iodide and soluble sulphides. *Anal. Chim. Acta* **1970**, *50*, 299–303.
- (6) Forbes, W. F.; Hamlin, C. R. Determination of –SS and –SH groups in proteins. I. A reassessment of the use of methylmercuric iodide. *Can. J. Chem.* **1968**, *46*, 3033–3040.
- (7) Anderson, W. L.; Wetlaufer, D. B. A new method for the disulfide analysis of peptides. *Anal. Biochem.* **1975**, *67*, 493–502.
- (8) Chen, R. F. Measurements of absolute values in biochemical fluorescence spectroscopy. *J. Res. Natl. Bur. Stand.* **1972**, *76A* (6), 593–606.
- (9) Sponer, H. Remarks on the absorption spectra of phenylalanine and tyrosine in connection with the absorption in toluene and paracresol. *J. Chem. Phys.* **1942**, *10*, 672.
- (10) Kuipers, B. J.; Gruppen, H. Prediction of molar extinction coefficients of proteins and peptides using UV absorption of the constituent amino acids at 214 nm to enable quantitative reverse phase high-performance liquid chromatography-mass spectrometry analysis. *J. Agric. Food Chem.* **2007**, *55*, 5445–5451.
- (11) Aebi, U.; Pollard, T. D. A glow discharge unit to render electron microscope grids and other surfaces hydrophilic. *J. Electron Microsc. Technol.* **1987**, *7*, 29–33.
- (12) Utsunomiya, S.; Ewing, R. C. Application of high-angle annular dark field scanning transmission electron microscopy, scanning transmission electron microscopy-energy dispersive X-ray spectrometry, and energy-filtered transmission electron microscopy to the characterization of nanoparticles in the environment. *Environ. Sci. Technol.* **2003**, *37*, 786–791.
- (13) Savitzky, A.; Golay, M. J. E. Smoothing and differentiation of data by simplified least squares procedures. *Anal. Chem.* **1964**, *36*, 1627–1639.
- (14) Hughes, R. M.; Waters, M. L. Model systems for  $\beta$ -hairpins and  $\beta$ -sheets. *Curr. Opin. Struct. Biol.* **2006**, *16*, 514–524.
- (15) Dong, A.; Hoang, P.; Caughey, W. S. Protein secondary structures in water from second-derivative amide I infrared spectra. *Biochemistry* **1990**, *29*, 3303–3308.
- (16) Matsushima, N.; Yoshida, H.; Kumaki, Y.; Kamiya, M.; Tanaka, T.; Izumi, Y.; Kretsinger, R. H. Flexible structures and ligand interactions of tandem repeats consisting of proline, glycine, asparagine, serine, and/or threonine rich oligopeptides in proteins. *Curr. Protein Pept. Sci.* **2008**, *9*, 591–610.
- (17) Blanco, F.; Ramirez-Alvarado, M.; Serrano, L. Formation and stability of beta-hairpin structures in polypeptides. *Curr. Opin. Struct. Biol.* **1998**, *8*, 107–111.
- (18) Rose, G. D.; Gierasch, L. M.; Smith, J. A. Turns in peptides and proteins. *Adv. Protein Chem.* **1985**, *37*, 1–109.
- (19) Chou, P. Y.; Fasman, G. D. Beta-turns in proteins. *J. Mol. Biol.* **1977**, *115*, 135–175.
- (20) Wilmot, C. M.; Thornton, J. M. Analysis and prediction of the different types of beta-turn in proteins. *J. Mol. Biol.* **1988**, *203*, 221–232.
- (21) Whitesides, G. M.; Mathias, J. P.; Seto, C. T. Molecular self-assembly and nanochemistry: a chemical strategy for the synthesis of nanostructures. *Science* **1991**, *254*, 1312–1319.
- (22) Sukthankar, P.; Avila, L. A.; Whitaker, S. K.; Iwamoto, T.; Morgenstern, A.; Apostolidis, C.; Liu, K.; Hanzlik, R. P.; Dadachova, E.; Tomich, J. M. Branched amphiphilic peptide capsules: cellular uptake and retention of encapsulated solutes. *Biochim. Biophys. Acta, Biomembr.* **2014**, *1838*, 2296–2305.
- (23) Kannan, N.; Vishveshwara, S. Aromatic clusters: a determinant of thermal stability of thermophilic proteins. *Protein Eng.* **2000**, *13*, 753–761.
- (24) Serrano, L.; Bycroft, M.; Fersht, A. R. Aromatic-aromatic interactions and protein stability. Investigation by double-mutant cycles. *J. Mol. Biol.* **1991**, *218*, 465–475.
- (25) Gao, H.; Shi, W.; Freund, L. B. Mechanics of receptor-mediated endocytosis. *Proc. Natl. Acad. Sci. U. S. A.* **2005**, *102*, 9469–9474.
- (26) Win, K. Y.; Feng, S. S. Effects of particle size and surface coating on cellular uptake of polymeric nanoparticles for oral delivery of anticancer drugs. *Biomaterials* **2005**, *26*, 2713–2722.
- (27) Kulkarni, S. A.; Feng, S. S. Effects of particle size and surface modification on cellular uptake and biodistribution of polymeric nanoparticles for drug delivery. *Pharm. Res.* **2013**, *30*, 2512–2522.